2006

Bayesian Defect Signal Analysis

Aleksandar Dogandžić
Iowa State University, ald@iastate.edu

Benhong Zhang
Iowa State University

Bayesian Defect Signal Analysis

Abstract
We develop a Bayesian framework for estimating defect signals from noisy measurements. We propose a parametric model for the shape of the defect region and assume that the defect signal within this region is random with unknown mean and variance. Markov chain Monte Carlo (MCMC) algorithms are derived for simulating from the posterior distributions of the model parameters and defect signals. These algorithms are utilized to identify potential defect regions and estimate their size and reflectivity. We specialize the proposed framework to elliptical defect shape and Gaussian signal and noise models and apply it to experimental ultrasonic *C*-scan data from an inspection of a cylindrical titanium billet.

Keywords
Bayesian analysis, defect estimation and detection, Markov chain Monte Carlo (MCMC)

Disciplines
Applied Statistics | Electrical and Computer Engineering | Numerical Analysis and Computation | Signal Processing

Comments
The following article appeared in *AIP Conference Proceedings* 820 (2006): 820 and may be found at doi:10.1063/1.2184584.

Bayesian Defect Signal Analysis

Aleksandar Dogandži and Benhong Zhang

Citation: AIP Conference Proceedings **820**, 617 (2006); doi: 10.1063/1.2184584
View online: http://dx.doi.org/10.1063/1.2184584
View Table of Contents:
http://scitation.aip.org/content/aip/proceeding/aipcp/820?ver=pdfcov
Published by the AIP Publishing

BAYESIAN DEFECT SIGNAL ANALYSIS

Aleksandar Dogandžić and Benhong Zhang

Iowa State University, Center for Nondestructive Evaluation,
1915 Scholl Road, Ames, IA 50011, USA

ABSTRACT. We develop a Bayesian framework for estimating defect signals from noisy measurements. We propose a parametric model for the shape of the defect region and assume that the defect signal within this region is random with unknown mean and variance. Markov chain Monte Carlo (MCMC) algorithms are derived for simulating from the posterior distributions of the model parameters and defect signals. These algorithms are utilized to identify potential defect regions and estimate their size and reflectivity. We specialize the proposed framework to elliptical defect shape and Gaussian signal and noise models and apply it to experimental ultrasonic C-scan data from an inspection of a cylindrical titanium billet.

Keywords: Bayesian analysis, defect estimation and detection, Markov chain Monte Carlo (MCMC).
PACS: 02.50.Tt Inference methods, 02.50.Ng Distribution theory and Monte Carlo studies.

INTRODUCTION

In NDE applications, defect signal typically affects multiple measurements at neighboring spatial locations. Therefore, multiple spatial measurements should be incorporated into defect detection and estimation (sizing) algorithms. In this paper (see also [1]), we propose a *parametric model* for defect shape, location, and reflectivity, a *Bayesian framework* for estimating these parameters, and a sequential method for identifying multiple defect regions and estimating their parameters. We adopt elliptical defect shape and Gaussian signal and noise models; however, the proposed framework is applicable to other scenarios as well. The elliptical shape model is well-suited for describing hard alpha inclusions in titanium alloys [2]. In most applications, the defect signal is not uniform over the defect region but varies *randomly* depending, for example, on local reflectivity and various constructive and destructive interferences. To account for these variations, we assume that the defect signal is *random* over the defect region, having a fixed but unknown mean and unknown variance. Our approach provides estimates and Bayesian confidence intervals for the unknown defect parameters. Furthermore, the underlying Bayesian paradigm allows us to easily incorporate available prior information about the defect signal, shape, or size.

We first introduce the measurement model and prior specifications. We then develop Bayesian methods for estimating the defect model parameters and defect signals. The proposed methods are applied to experimental ultrasonic C-scan data from an inspection of a cylindrical titanium billet.

CP820, *Review of Quantitative Nondestructive Evaluation Vol. 25,* ed. by D. O. Thompson and D. E. Chimenti

MEASUREMENT MODEL AND PRIOR SPECIFICATIONS

In this section, we first introduce our parametric defect location and shape models and describe the random noise and defect-signal models. Then, we combine the nose and signal models by integrating out the random signals. Finally, we introduce the prior specifications employed in this paper.

Parametric Model for Defect Location and Shape

Assume that a potential defect-signal region $\mathcal{R}(\boldsymbol{z})$ can be modeled as an ellipse:

$$\mathcal{R}(\boldsymbol{z}) = \{\boldsymbol{r} : (\boldsymbol{r} - \boldsymbol{r}_0)^T \Sigma_{\mathrm{R}}^{-1} (\boldsymbol{r} - \boldsymbol{r}_0) \leq 1\} \tag{1}$$

where $\boldsymbol{r} = [x_1, x_2]^T$ denotes location in Cartesian coordinates,

$$\boldsymbol{z} = [\boldsymbol{r}_0^T, d, A, \varphi]^T \tag{2}$$

is the vector of (unknown) defect location and shape parameters,

$$\Sigma_{\mathrm{R}} = \begin{bmatrix} \cos\varphi & -\sin\varphi \\ \sin\varphi & \cos\varphi \end{bmatrix} \cdot \begin{bmatrix} d^2 & 0 \\ 0 & A^2/(d^2\pi^2) \end{bmatrix} \cdot \begin{bmatrix} \cos\varphi & -\sin\varphi \\ \sin\varphi & \cos\varphi \end{bmatrix}^T \tag{3}$$

and "^{T}" denotes a transpose. Here, $\boldsymbol{r}_0 = [x_{0,1}, x_{0,2}]^T$ is the center of the ellipse in Cartesian coordinates, $d > 0$ is an axis parameter, A the area of the ellipse, and $\varphi \in [-\pi/4, \pi/4]$ the ellipse orientation parameter (in radians). Under the above parametrization, d and $A/(d\pi)$ are the axes of the ellipse $\mathcal{R}(\boldsymbol{z})$.

Measurement-Error (Noise) Model

Assume that we have collected measurements y_i at locations $\boldsymbol{s}_i$, $i = 1, 2, \ldots, N$. We adopt the following measurement-error model:

- If y_i is collected over the defect region [i.e. $\boldsymbol{s}_i \in \mathcal{R}(\boldsymbol{z})$], then

$$y_i = \theta_i + e_i \tag{4a}$$

  where θ_i and e_i are the defect signal (related to its reflectivity) and noise at location s_i;

- if y_i is collected outside the defect region [i.e. $\boldsymbol{s}_i \in \mathcal{R}^{\mathrm{c}}(\boldsymbol{z})$, where $\mathcal{R}^{\mathrm{c}}(\boldsymbol{z})$ denotes the *noise-only region* outside $\mathcal{R}(\boldsymbol{z})$], then the measurements contain only noise:

$$y_i = e_i. \tag{4b}$$

Note that (4b) follows by setting $\theta_i = 0$ in (4a). We model the additive noise samples e_i, $i = 1, 2, \ldots, N$ as zero-mean independent, identically distributed (i.i.d.) Gaussian random variables with known variance σ^2 (which can be easily estimated from the noise-only data). Let us denote by $\mathcal{N}(y; \mu, \sigma^2)$ the Gaussian probability density function (pdf) of a random variable y with mean μ and variance σ^2. Then, (4a) and (4b) imply that the conditional distribution of the measurement y_i given θ_i is

$$p(y_i \,|\, \theta_i) = \mathcal{N}(y_i; \theta_i, \sigma^2), \quad i = 1, 2, \ldots, N \tag{5}$$

where $\theta_i = 0$ for $\boldsymbol{s}_i \in \mathcal{R}^{\mathrm{c}}(\boldsymbol{z})$. In the following discussion, we describe a model for the signal θ_i within the defect region $\mathcal{R}(\boldsymbol{z})$.

Defect-Signal (Reflectivity) Model

Assume that the defect signals $\{\theta_i,\ \boldsymbol{s}_i \in \mathcal{R}(\boldsymbol{z})\}$ are i.i.d. Gaussian with unknown mean μ and variance τ^2, which define the vector of unknown defect-signal parameters:

$$\boldsymbol{w} = [\mu, \tau]^T. \tag{6}$$

Therefore, the joint pdf of the defect signals conditional on $\boldsymbol{w}$ and $\boldsymbol{z}$ can be written as

$$p(\{\theta_i,\ \boldsymbol{s}_i \in \mathcal{R}(\boldsymbol{z})\} \,|\, \boldsymbol{z}, \boldsymbol{w}) = \prod_{i,\ \boldsymbol{s}_i \in \mathcal{R}(\boldsymbol{z})} \mathcal{N}(\theta_i; \mu, \tau^2). \tag{7}$$

Note that the defect-signal standard deviation τ is a measure of defect-signal variability; if $\tau = 0$, then all θ_i within the defect region are *equal to* μ.

Measurement Model for Estimating the Defect-Signal and Shape Parameters

Define the vector of all model (defect-signal, location, and shape) parameters $\boldsymbol{\phi} = [\boldsymbol{z}^T, \boldsymbol{w}^T]^T$, see also (2) and (6). We now combine the noise and defect-signal models and *integrate out* the θ_is. Consequently, conditional on the model parameters $\boldsymbol{\phi}$, the observations y_i collected over the defect region are i.i.d. Gaussian random variables with the pdf:

$$p(y_i \,|\, \boldsymbol{\phi}) = \mathcal{N}(y_i; \mu, \sigma^2 + \tau^2), \quad \text{for } \boldsymbol{s}_i \in \mathcal{R}(\boldsymbol{z}) \tag{8a}$$

whereas the observations collected in the noise-only region are zero-mean conditionally i.i.d. Gaussian with pdf:

$$p(y_i \,|\, \boldsymbol{\phi}) = \mathcal{N}(y_i; 0, \sigma^2), \quad \text{for } \boldsymbol{s}_i \in \mathcal{R}^{\mathrm{c}}(\boldsymbol{z}). \tag{8b}$$

Prior Specifications

We assume that defect location, shape, and signal parameters are independent *a priori*:

$$\pi_{\boldsymbol{\phi}}(\boldsymbol{\phi}) = \pi_{\boldsymbol{z}}(\boldsymbol{z}) \cdot \pi_{\boldsymbol{w}}(\boldsymbol{w}) \tag{9a}$$

where

$$\pi_{\boldsymbol{z}}(\boldsymbol{z}) = \pi_{x_{0,1}}(x_{0,1}) \cdot \pi_{x_{0,2}}(x_{0,2}) \cdot \pi_d(d) \cdot \pi_A(A) \cdot \pi_\varphi(\varphi) \tag{9b}$$

$$\pi_{\boldsymbol{w}}(\boldsymbol{w}) = \pi_\mu(\mu) \cdot \pi_\tau(\tau). \tag{9c}$$

Here, $\pi_{\boldsymbol{\phi}}(\boldsymbol{\phi})$ denotes the prior pdf of $\boldsymbol{\phi}$ and analogous notation is used for the prior pdfs of the components of $\boldsymbol{\phi}$. Let us adopt simple uniform-distribution priors for all the model parameters:

$$\pi_\mu(\mu) = \mathrm{uniform}(0, \mu_{\mathrm{MAX}}), \quad \pi_\tau(\tau) = \mathrm{uniform}(0, \tau_{\mathrm{MAX}}) \tag{10a}$$

$$\pi_{x_{0,1}}(x_{0,1}) = \mathrm{uniform}(x_{0,1,\mathrm{MIN}}, x_{0,1,\mathrm{MAX}}), \quad \pi_{x_{0,2}}(x_{0,2}) = \mathrm{uniform}(x_{0,2,\mathrm{MIN}}, x_{0,2,\mathrm{MAX}}) \tag{10b}$$

$$\pi_d(d) = \mathrm{uniform}(d_{\mathrm{MIN}}, d_{\mathrm{MAX}}), \quad \pi_A(A) = \mathrm{uniform}(A_{\mathrm{MIN}}, A_{\mathrm{MAX}}), \tag{10c}$$

$$\pi_\varphi(\varphi) = \mathrm{uniform}(\varphi_{\mathrm{MIN}}, \varphi_{\mathrm{MAX}}) \tag{10d}$$

where $\varphi_{\mathrm{MIN}} \geq -\pi/4$ and $\varphi_{\mathrm{MAX}} \leq \pi/4$.

BAYESIAN ANALYSIS

We now develop Bayesian methods for estimating the model parameters $\boldsymbol{\phi}$ and random signals θ_i, $i = 1, 2, \ldots, N$. The posterior distribution of the model parameters $\boldsymbol{\phi}$ follows by using (8a)–(8b) and (9a); it is given by (up to a proportionality constant):

$$p(\boldsymbol{\phi} \,|\, \boldsymbol{y}) \ \propto\ \pi_{\boldsymbol{z}}(\boldsymbol{z}) \cdot \pi_{\boldsymbol{w}}(\boldsymbol{w}) \cdot l(\boldsymbol{y} \,|\, \boldsymbol{z}, \boldsymbol{w}) \tag{11a}$$

where $\boldsymbol{y} = [y_1, y_2, \ldots, y_N]^T$ denotes the vector of all observations and

$$\begin{aligned} l(\boldsymbol{y} \,|\, \boldsymbol{z}, \boldsymbol{w}) &= \prod_{i,\, \boldsymbol{s}_i \in \mathcal{R}(\boldsymbol{z})} \frac{\mathcal{N}(y_i; \mu, \sigma^2 + \tau^2)}{\mathcal{N}(y_i; 0, \sigma^2)} \\ &= \left(1 + \frac{\tau^2}{\sigma^2}\right)^{-N(\boldsymbol{z})/2} \cdot \exp\left\{ -\tfrac{1}{2} \sum_{i,\, \boldsymbol{s}_i \in \mathcal{R}(\boldsymbol{z})} \left[\frac{(y_i - \mu)^2}{\sigma^2 + \tau^2} - \frac{y_i^2}{\sigma^2} \right] \right\}. \quad (11b) \end{aligned}$$

Estimation of the Model Parameters

We outline our proposed scheme for simulating from the joint posterior pdf $p(\boldsymbol{\phi} \,|\, \boldsymbol{y})$. To simulate samples from this distribution, we apply the Gibbs sampler [4] which utilizes the full conditional posterior pdfs of τ, μ and $\boldsymbol{z}$:

1) Draw $\tau^{(t)}$ from

$$\begin{aligned} &p(\tau \,|\, \mu^{(t-1)}, \boldsymbol{z}^{(t-1)}, \boldsymbol{y}) \\ &\quad \propto (\sigma^2 + \tau^2)^{-N(\boldsymbol{z}^{(t-1)})/2} \cdot \exp\left[- \frac{\sum_{i,\, \boldsymbol{s}_i \in \mathcal{R}(\boldsymbol{z}^{(t-1)})} (y_i - \mu^{(t-1)})^2}{2\,(\sigma^2 + \tau^2)} \right] \cdot i_{(0, \tau_{\mathrm{MAX}})}(\tau) \quad (12a) \end{aligned}$$

using *rejection sampling*, where $\mu^{(t-1)}$ and $\boldsymbol{z}^{(t-1)}$ have been obtained in Steps 2) and 3) of the $(t-1)$th cycle, $i_A(x) = \begin{cases} 1, & x \in A, \\ 0, & \text{otherwise} \end{cases}$ denotes the indicator function, and $N(\boldsymbol{z}) = \sum_{i,\, \boldsymbol{s}_i \in \mathcal{R}(\boldsymbol{z})} 1$ denotes the number of measurements collected over $\mathcal{R}(\boldsymbol{z})$.

2) Draw $\mu^{(t)}$ from

$$p(\mu \,|\, \tau^{(t)}, \boldsymbol{z}^{(t-1)}, \boldsymbol{y}) \propto \mathcal{N}\Big(\mu\,;\, \overline{y}(\boldsymbol{z}^{(t-1)}), \frac{\sigma^2 + (\tau^{(t)})^2}{N(\boldsymbol{z}^{(t-1)})}\Big) \cdot i_{(0, \mu_{\mathrm{MAX}})}(\mu) \quad (12b)$$

which is a *truncated Gaussian distribution*, easy to sample from using e.g. the algorithm in [3]. Here,

$$\overline{y}(\boldsymbol{z}) = \frac{1}{N(\boldsymbol{z})} \sum_{i,\, \boldsymbol{s}_i \in \mathcal{R}(\boldsymbol{z})} y_i \quad (12c)$$

is the sample mean of the measurements collected over the defect region $\mathcal{R}(\boldsymbol{z})$.

3) Draw $\boldsymbol{z}^{(t)}$ from

$$p(\boldsymbol{z} \,|\, \boldsymbol{w}^{(t)}, \boldsymbol{y}) \propto \pi_{\boldsymbol{z}}(\boldsymbol{z}) \cdot l(\boldsymbol{y} \,|\, \boldsymbol{z}, \boldsymbol{w}^{(t)}) \quad \text{where} \quad \boldsymbol{w}^{(t)} = [\mu^{(t)}, \tau^{(t)}]^T \quad (12d)$$

using *shrinkage slice sampling* [5].

Cycling through the Steps 1)–3) is performed until the desired number of samples $\boldsymbol{\phi}^{(t)} = [(\boldsymbol{z}^{(t)})^T, (\boldsymbol{w}^{(t)})^T]^T$ is collected (after discarding the samples from the burn-in period, see e.g. [4]). Details of Steps 1)–3) will be given in [1]. This scheme produces a *Markov chain* $\boldsymbol{\phi}^{(0)}, \boldsymbol{\phi}^{(1)}, \boldsymbol{\phi}^{(2)}, \ldots$ with stationary distribution equal to the posterior pdf $p(\boldsymbol{\phi} \,|\, \boldsymbol{y})$.

Estimation of the Random Signals $\boldsymbol{\theta_i}$

To estimate the random signals $\boldsymbol{\theta} = [\theta_1, \theta_2, \ldots, \theta_N]^T$ we need to sample from its posterior (predictive) pdf

$$p(\boldsymbol{\theta} \,|\, \boldsymbol{y}) = \int p(\boldsymbol{\theta} \,|\, \boldsymbol{\phi}, \boldsymbol{y})\, p(\boldsymbol{\phi} \,|\, \boldsymbol{y})\, d\boldsymbol{\phi} \quad (13)$$

which can be done as follows:

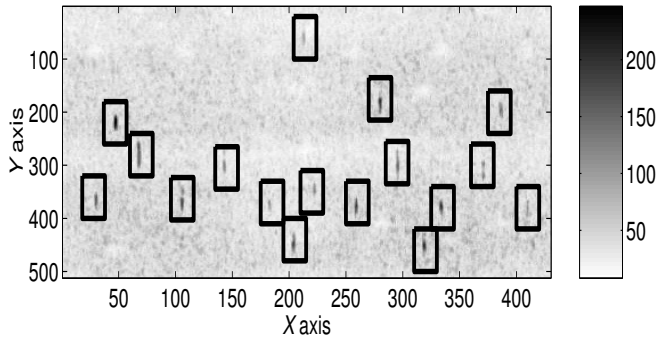

FIGURE 1. Ultrasonic C-scan data with 17 defects.

- Draw $\boldsymbol{\phi}^{(t)}$ from $p(\boldsymbol{\phi} \,|\, \boldsymbol{y})$, as outlined in the previous section;
- Draw $\boldsymbol{\theta}^{(t)}$ from $p(\boldsymbol{\theta} \,|\, \boldsymbol{\phi}^{(t)}, \boldsymbol{y})$ as follows:
  - for $i \in \mathcal{R}(\boldsymbol{z}^{(t)})$, draw conditionally independent samples $\theta_i^{(t)}$ from

$$\mathcal{N}\Big(\theta_i^{(t)}, \frac{(\tau^{(t)})^2\, y_i + \sigma^2\, \mu^{(t)}}{(\tau^{(t)})^2 + \sigma^2}, \Big[\frac{1}{(\tau^{(t)})^2} + \frac{1}{\sigma^2}\Big]^{-1}\Big) \tag{14a}$$

  - for $i \in \mathcal{R}^{\mathrm{c}}(\boldsymbol{z}^{(t)})$, set

$$\theta_i^{(t)} = 0 \tag{14b}$$

yielding $\boldsymbol{\theta}^{(t)} = [\theta_1^{(t)}, \theta_2^{(t)}, \ldots, \theta_N^{(t)}]^T$.

Then, the posterior predictive estimate of the mean defect signal based on the defect-signal and model-parameter samples $\boldsymbol{\theta}^{(t)}$ and $\boldsymbol{\phi}^{(t)}$ is:

$$\overline{\theta}^{(t)} = \frac{1}{N(\boldsymbol{z}^{(t)})} \sum_{i,\, \boldsymbol{s}_i \in \mathcal{R}(\boldsymbol{z}^{(t)})} \theta_i^{(t)}. \tag{15}$$

Note that the proposed Markov chain Monte Carlo (MCMC) algorithms are *automatic*, i.e. their implementation does not require preliminary runs and additional tuning.

NUMERICAL EXAMPLES

We apply the proposed approach to experimental ultrasonic C-scan data from an inspection of a cylindrical Ti 6-4 billet. The sample, taken from the contaminated billet, contains 17 # 2 flat bottom holes at 3.2" depth. The ultrasonic data were collected in a single experiment by moving a probe along the axial direction and scanning the billet along the circumferential direction at each axial position. The raw C-scan data with marked defects are shown in Fig. 1. The vertical coordinate is proportional to rotation angle and the horizontal coordinate to axial position.

Before analyzing the data, we divided the C-scan image into three regions, as shown in Fig. 2. In each region, we subtracted row means from the measurements within the same row. We note that the noise level in Region 2 is lower than the corresponding noise levels in Regions 1 and 3. Indeed, the sample estimates of the noise variance σ^2 in Regions

1,2, and 3 are: $\sigma^2 = 11.9^2, 10.3^2$, and 12.0^2 (respectively). The underlying non-stationarity of the noise is due to the billet manufacturing process. We now analyze each region separately assuming known noise variances σ^2, given above. We chose the prior pdfs in (10) with $\mu_{\text{MAX}} = \max\{y_1, y_2, \ldots, y_N\}, \tau_{\text{MAX}} = 3\,\sigma, d_{\text{MIN}} = 1, d_{\text{MAX}} = 10, A_{\text{MIN}} = 30, A_{\text{MAX}} = 300, \varphi_{\text{MIN}} = -\pi/8, \varphi_{\text{MAX}} = \pi/8$, and selected $x_{0,i,\text{MIN}}, x_{0,i,\text{MAX}}, i = 1, 2$ according to the region that is being analyzed.

We now describe our analysis of Region 1, where we ran seven Markov chains. We perform *sequential identification* of potential defects, as described in the following discussion. We first ran $10,000$ cycles of the proposed Gibbs sampler and utilized the last $T = 2,000$ samples to estimate the posterior distributions $p(\boldsymbol{\phi} \,|\, \boldsymbol{y})$ and $p(\boldsymbol{\theta} \,|\, \boldsymbol{y})$, implying that the burn-in period is $t_0 = 8,000$ samples. The posterior means $\mathrm{E}\,[\theta_i \,|\, \boldsymbol{y}]$ of the random signals θ_i, which are also the minimum mean-square error (MMSE) estimates of θ_i, have been estimated by averaging the T draws:

$$\widehat{\theta}^{(1)}_{i,\text{MMSE}} \approx \frac{1}{T} \sum_{t=t_0+1}^{t_0+T} \theta_i^{(t)}, \quad i = 1, 2, \ldots, N. \tag{16}$$

Before running the second chain, we *subtracted* the first chain's MMSE estimates $\widehat{\theta}^{(1)}_{i,\text{MMSE}}$ from the measurements y_i, $i = 1, 2, \ldots, N$, effectively removing the first potential defect region from the data. We then ran the second Markov chain using the filtered data $y_i^{(2)} = y_i - \widehat{\theta}^{(1)}_{i,\text{MMSE}}$, computed the MMSE estimates $\widehat{\theta}^{(2)}_{i,\text{MMSE}}$ of the second potential defect signal, subtracted them out (yielding $y_i^{(3)} = y_i^{(2)} - \widehat{\theta}^{(2)}_{i,\text{MMSE}}$), and continued this procedure until reaching the desired number of chains. In Fig. 3 (a), we show average log posterior pdfs (up to an additive constant) of the seven potential defects, computed using the logarithms of the right-hand sides of (11a), averaged over the last T draws. The chains have been sorted in the decreasing order according to their average log posterior pdfs. Note that the average log posterior curve flattens out for indices higher than five. Hence, we focus on the first five chains in Region 1.

We have applied the above sequential scheme to Regions 2 and 3, where we ran seven and ten chains, respectively. The obtained average log posterior pdfs (up to an additive constant) for these chains are shown in Figs. 3 (b) and 3 (c). For Regions 2 and 3, the average log posterior curves flatten out for indices higher than five and seven. Hence, we focus on the first five chains in Region 2 and first seven chains in region 3.

Fig. 2 shows the MMSE estimates (16) of the defect signals in the first five potential defects (chains) from Region 1, and first five and seven potential defects from Regions 2 and 3, respectively. The ranks (chain indices) of the potential defects within each region are also shown in Fig. 2. Remarkably, the locations of these 17 potential defects correspond to the true locations of the flat bottom holes (i.e. the true defects) in Fig. 1.

We now show estimated mean-signal posterior distributions of the potential defects in the lower right part of Region 3. Fig. 4 shows

- the measurements in this sub-region (after subtracting the row means) and
- the MMSE estimates (16) of the potential defect signals (with chain indices between five and nine) located in this sub-region.

Here, the fifth, sixth, and seventh chains correspond to the real defects, see also Figs. 1 and 2. In Fig. 5, we show an estimated marginal posterior pdf of the mean defect signal $\overline{\theta}$ [computed using (15)] for the potential defect signals with chain indices 7, 8, and 9. Interestingly, the 9th potential defect region (chain) has a slightly higher mean signal $\overline{\theta}$ than the 7th region.

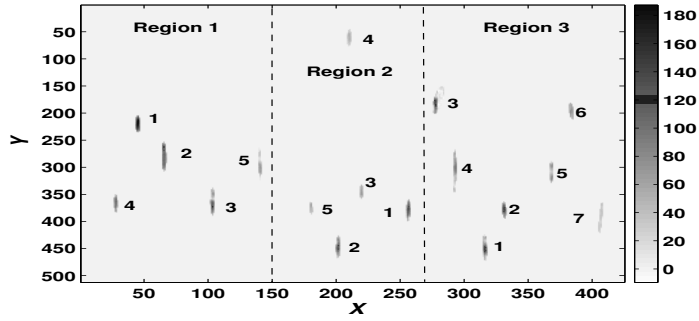

FIGURE 2. Defect estimation results: MMSE estimates (16) of the defect signals for the chains having the largest average log posterior pdfs.

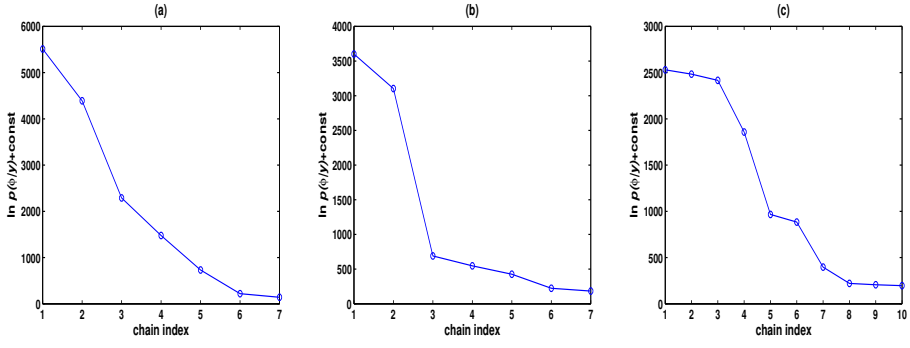

FIGURE 3. Average log posterior pdfs of the potential defects (up to an additive constant) in Region 1,2, and 3, respectively.

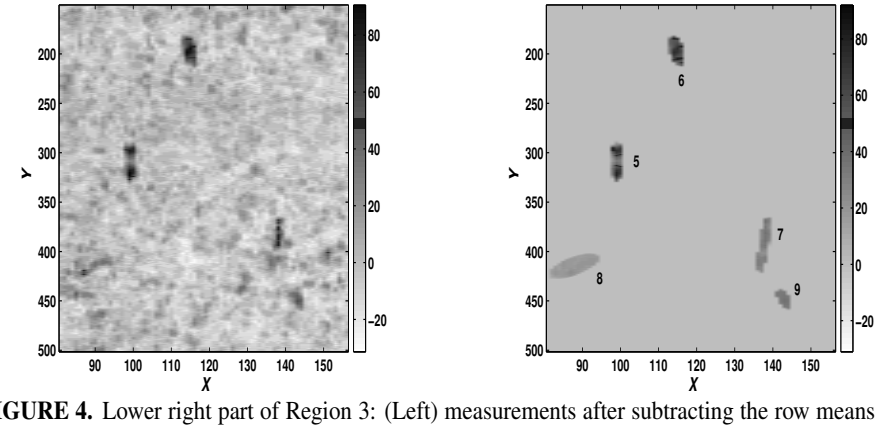

FIGURE 4. Lower right part of Region 3: (Left) measurements after subtracting the row means and (Right) MMSE estimates of the potential defect signals 5–9.

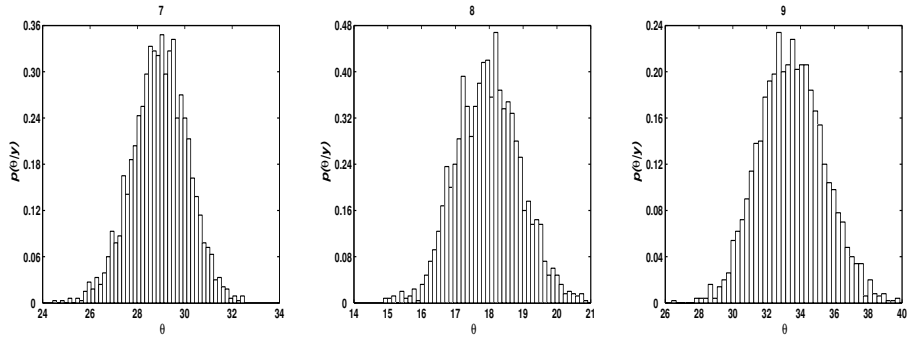

FIGURE 5. Estimated marginal posterior pdfs of the mean defect signal $\overline{\theta}$ for chains 7, 8, and 9 in Region 3.

However, its area is significantly smaller than that of the 7th region, which explains why the 7th chain (which corresponds to a true defect) achieves a higher average log posterior pdf.

CONCLUDING REMARKS

We developed a Bayesian framework for detecting and estimating NDE defect signals from noisy measurements, derived MCMC methods for estimating the defect signal, location, and shape parameters, and successfully applied them to experimental ultrasonic C-scan data. Our algorithms are automatic and remarkably easy to implement, requiring only sampling from univariate Gaussian, uniform, and exponential distributions. Further research will include generalizing the proposed approach to account for correlated noise.

ACKNOWLEDGMENTS

This work was supported by the NSF Industry-University Cooperative Research Program, Center for Nondestructive Evaluation (CNDE), Iowa State University. We are grateful to Dr. R. B. Thompson from CNDE for his insightful comments and for bringing reference [2] to our attention.

REFERENCES

1. Dogandžić A. and Zhang B., "Bayesian NDE defect signal analysis," in preparation.
2. Aerospace Industries Association Rotor Integrity Sub-Committee, "The development of anomaly distributions for aircraft engine titanium disk alloys," in *Proc. 38th AIAA/ASME/ASCE/AHS/ASC Structures, Structural Dynamics, and Materials Conf.,* Kissimmee, FL, Apr. 1997, pp. 2543–2553.
3. Geweke, J., "Efficient simulation from the multivariate normal and Student-t distributions subject to linear constraints," in *Computing Science and Statistics: Proc. 23rd Symposium on the Interface,* Seattle, WA, Apr. 1991, pp. 571–578.
4. Gelman, A., Carlin, J.B., Stern H.S., and Rubin D.B., *Bayesian Data Analysis*, 2nd. ed., New York: Chapman & Hall, 2004.
5. Neal R.M., "Slice sampling," *Ann. Statist.,* **31**, 705–741 (2003).